

# Tuberculosis from Head to Toe<sup>1</sup>

(CME available in print version and on RSNA Link)

## LEARNING OBJECTIVES

After reading this article and taking the test, the reader will be able to:

- Identify the radiologic features of diverse forms of tuberculosis affecting various organ systems.
- Explain how tuberculosis can mimic a variety of other disease entities at radiology.
- Define the role of current imaging modalities in diagnosing tuberculosis.

Mukesh G. Harisinghani, MD • Theresa C. McLoud, MD • Jo-Anne O. Shepard, MD • Jane P. Ko, MD • Manohar M. Shroff, MD • Peter R. Mueller, MD

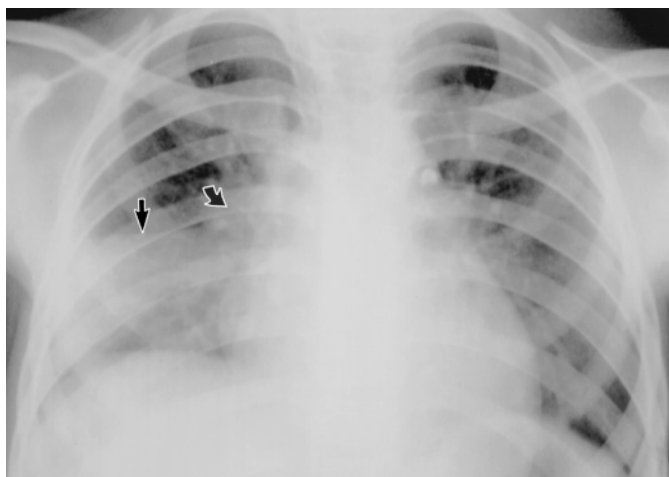
Tuberculosis can affect virtually any organ system in the body and can be devastating if left untreated. The increasing prevalence of tuberculosis in both immunocompetent and immunocompromised individuals in recent years makes this disease a topic of universal concern. Because tuberculosis demonstrates a variety of clinical and radiologic findings and has a known propensity for dissemination from its primary site, it can mimic numerous other disease entities. Primary pulmonary tuberculosis typically manifests radiologically as parenchymal disease, lymphadenopathy, pleural effusion, miliary disease, or lobar or segmental atelectasis. In postprimary tuberculosis, the earliest radiologic finding is the development of patchy, ill-defined segmental consolidation. Both computed tomography (CT) and magnetic resonance (MR) imaging are helpful in diagnosing tuberculous spondylitis and tuberculous arthritis. CT is especially useful in depicting gastrointestinal and genitourinary tuberculosis. In tuberculosis involving the central nervous system, CT and MR imaging findings vary depending on the stage of disease and the character of the lesion. A high degree of clinical suspicion and familiarity with the various radiologic manifestations of tuberculosis allow early diagnosis and timely initiation of appropriate therapy, thereby reducing patient morbidity.

**Abbreviation:** AIDS = acquired immunodeficiency syndrome

**Index terms:** Tuberculosis, central nervous system, 10.236, 30.236, 139.23, 139.251 • Tuberculosis, gastrointestinal, 70.23 • Tuberculosis, genitourinary, 80.23 • Tuberculosis, musculoskeletal, 30.231, 40.23 • Tuberculosis, pulmonary, 60.231, 60.232

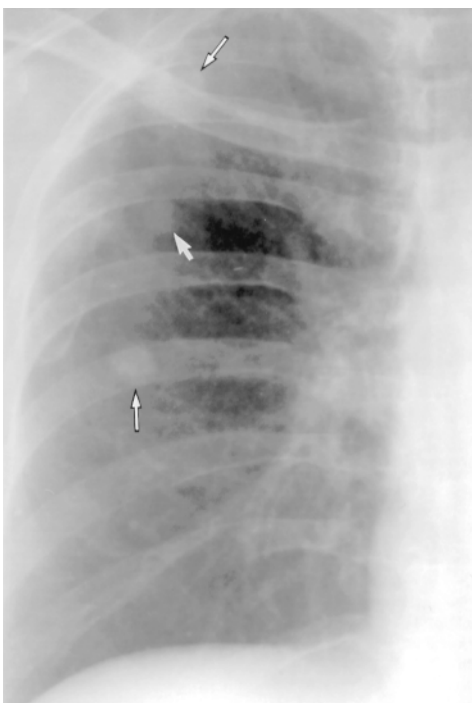
**RadioGraphics 2000; 20:449–470**

<sup>1</sup>From the Department of Radiology, Ellison 234, Massachusetts General Hospital, Harvard Medical School, 32 Fruit St, Boston, MA 02114 (M.G.H., T.C.M., J.O.S., J.P.K., P.R.M.), and the Department of Radiology, P.D. Hinduja National Hospital, Mahim, Bombay, India (M.M.S.). Presented as a scientific exhibit at the 1998 RSNA scientific assembly. Received February 19, 1999; revision requested April 14 and received June 18; accepted June 21. **Address reprint requests to** M.G.H. (e-mail: *mharisinghani@partners.org*).



1.

**Figures 1, 2.** (1) Consolidation in primary tuberculosis. Frontal chest radiograph demonstrates consolidation in the right middle lobe (straight arrow) with right hilar adenopathy (curved arrow). (2) Tuberculomas in primary tuberculosis. Frontal radiograph of the right lung demonstrates well-defined nodules (arrows), findings that are consistent with tuberculomas.



2.

## Introduction

Up until the mid 1980s, there was a steady decline in the prevalence of tuberculosis. Since that time, however, there has been a resurgence of tuberculosis due to the acquired immunodeficiency syndrome (AIDS) epidemic and the increasing number of drug-resistant strains of *Mycobacterium* tuberculosis (1). In addition to immunocompromised individuals, other population groups who are at increased risk include minorities, the poor, alcoholics, immigrants from third-world countries, prisoners, the aged, nursing home residents, and the homeless.

Although manifestations of tuberculosis are usually limited to the chest, the disease can affect any organ system and in patients infected with human immunodeficiency virus usually involves multiple extrapulmonary sites including the skeleton, genitourinary tract, and central nervous system.

Tuberculosis demonstrates a variety of clinical and radiologic features depending on the organ site involved and has a known propensity for dissemination from its primary site. Thus, tuberculosis can mimic a number of other disease entities, and it is important to be familiar with the various radiologic features of tuberculosis to ensure early, accurate diagnosis.

In this article, we discuss and illustrate the common imaging features of various types of tuberculosis affecting the lungs, heart, bones, joints, gas-

trointestinal system, genitourinary system, central nervous system, mastoid processes, and eyes.

## Pulmonary Tuberculosis

Pulmonary tuberculosis is classically divided into primary and postprimary (reactivation) tuberculosis. There is considerable overlap in the radiologic manifestations of these two entities.

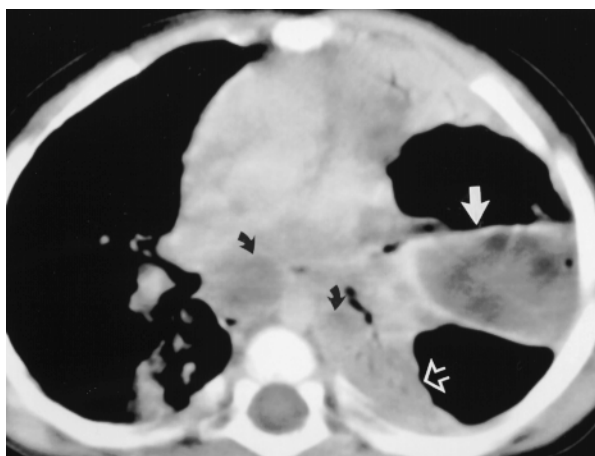
## Primary Tuberculosis

Although primary tuberculosis is the most common form of pulmonary tuberculosis in infants and children, it has been increasingly encountered in adult patients (2,3). Primary tuberculosis now accounts for 23%–34% of all adult cases of tuberculosis (4).

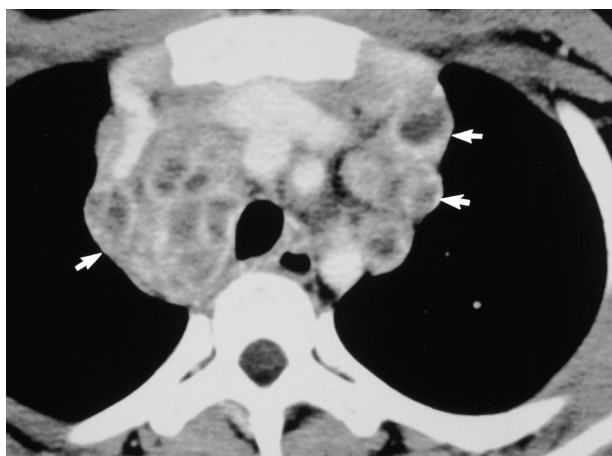
Primary tuberculosis typically manifests radiologically as parenchymal disease (Figs 1–3), lymphadenopathy (Fig 4), pleural effusion (Fig 5), miliary disease (Figs 6, 7), or atelectasis, which may be either lobar or segmental (5,6). However, results of chest radiography may be normal in 15% of cases (4).

Parenchymal disease in primary tuberculosis affects the areas of greatest ventilation; the most common sites are the middle lobe, the lower lobes, and the anterior segment of the upper lobes (5).

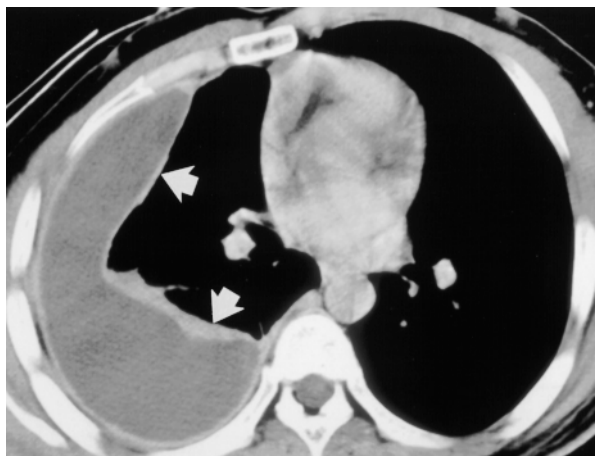
The radiologic differential diagnosis for tuberculous lymphadenopathy includes metastases and histoplasmosis in endemic areas. A radiologic



3.



4.



5.



6.

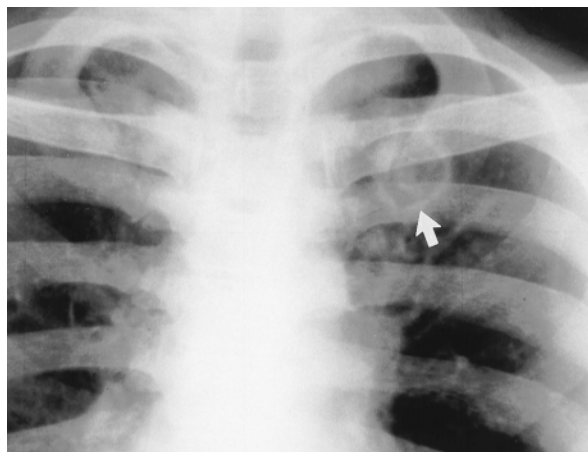


6.

finding of fine, discrete nodular areas of increased opacity is highly suggestive of tuberculosis in the appropriate clinical setting. However, it may also indicate varicella pneumonia, sarcoidosis, histoplasmosis, metastases, pneumoconiosis, or hemosiderosis.

**Figures 3–7.** (3) Pulmonary parenchymal changes and lymphadenopathy in primary tuberculosis. Axial contrast material-enhanced computed tomographic (CT) scan demonstrates a parenchymal lung cavity in the lingula (solid white arrow) with enlarged necrotic subcarinal lymph nodes (black arrows). There is accompanying collapse of the left lower lobe (open arrow). (4) Mediastinal tuberculous adenopathy. Axial contrast-enhanced CT scan demonstrates multiple enlarged mediastinal lymph nodes with central areas of low attenuation and peripheral enhancement (arrows). (5) Pleural effusion. Axial contrast-enhanced CT scan demonstrates a large, right-sided pleural collection. The enhancing parietal pleura is uniformly thickened (arrows). (6) Miliary tuberculosis. Frontal radiograph shows fine, discrete nodular areas of increased opacity bilaterally. (7) Miliary tuberculosis. High-resolution CT scan obtained with lung windowing demonstrates numerous fine, discrete nodules bilaterally in a random distribution.

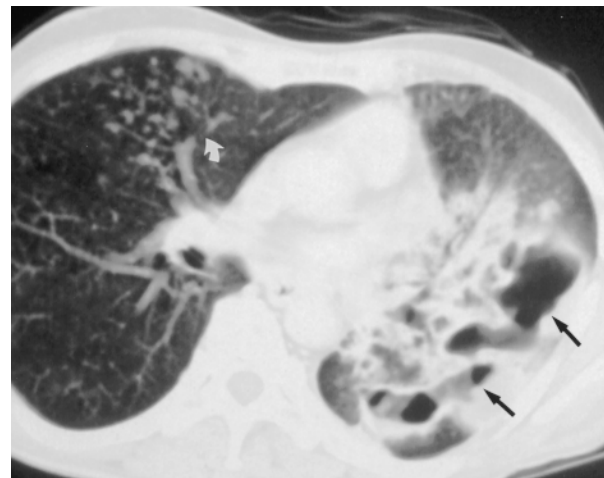
At CT, primary tuberculosis typically manifests as air-space consolidation that is dense, homogeneous, and well defined.



8.



9a.



9b.

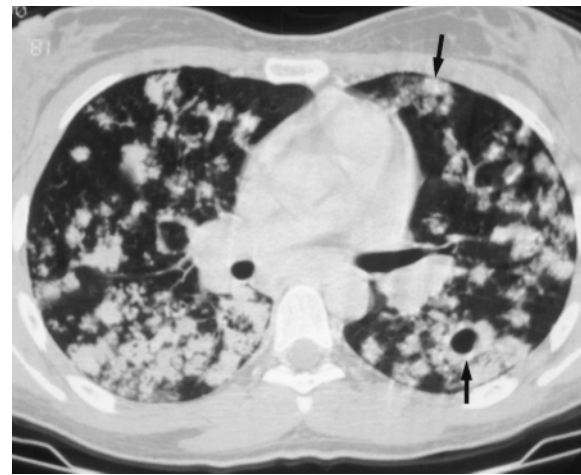


**Figure 10.** Fibroproliferative disease. Axial CT scan demonstrates bilateral diffuse, coarse, linear, and nodular areas of increased attenuation with cavitation (arrows).

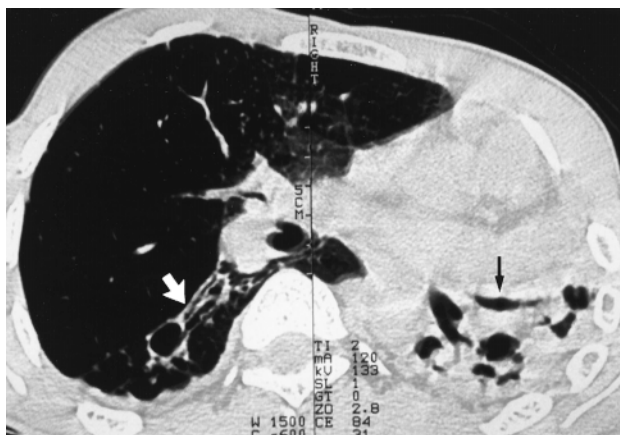
### Postprimary Tuberculosis

Postprimary disease results from reactivation of a previously dormant primary infection in 90% of cases; in a minority of cases, it represents continuation of the primary disease (7). Postprimary tuberculosis is almost exclusively a disease of adolescence and adulthood.

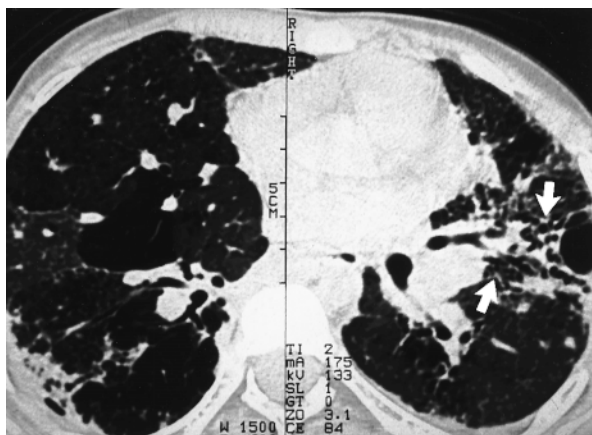
The radiologic features of postprimary tuberculosis can be broadly classified as parenchymal disease with cavitation, airway involvement, pleural extension, and other complications (3).

**Parenchymal Disease with Cavitation.**—The earliest radiologic finding in postprimary tuberculosis is the development of patchy, ill-defined segmental consolidation with a predilection for the apical or posterior segment of the upper lobes or the superior segment of the lower lobes (7,8). Two or more segments are involved in most cases, and bilateral upper lobe disease may be present.

Persistent masslike lesions, or tuberculomas, are an uncommon parenchymal manifestation of tuberculosis (5).



12.



13.

**Figures 12, 13.** (12) Lung destruction in postprimary tuberculosis. Axial CT scan demonstrates a fibrotic, shrunken left lung with compensatory overexpansion of the right lung extending across the midline. Bronchiectatic changes are noted bilaterally (arrows). (13) Bronchiectasis in postprimary tuberculosis. Axial CT scan demonstrates bronchiectasis in the left lung (arrows) with areas of emphysema.

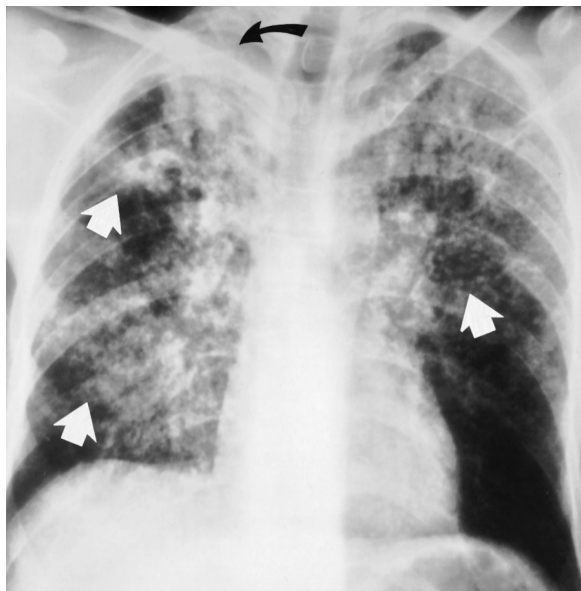


**Figure 11.** Fibroproliferative disease. Frontal chest radiograph shows clumped nodular and linear areas of increased opacity in both upper lobes and in the right middle lobe (white arrows). There is accompanying volume loss in the right upper lobe as well as overlying apical pleural thickening (black arrow).

Tuberculous cavitation most commonly occurs within areas of consolidation and indicates a high likelihood of activity. Cavities are often multiple and demonstrate thick, irregular walls (Figs 8, 9) (2,9). Air-fluid levels are rare, but when present they suggest the possibility of superinfection (4,10).

If left untreated, the disease progresses to lobar or complete lung opacification and destruction. In most cases, however, the initial heterogeneous areas of increased opacity evolve into more clearly defined, medium to coarse reticular and nodular opacified areas (fibroproliferative disease) (Figs 10, 11). These fibroproliferative lesions are most commonly seen in association with poorly marginated areas of increased opacity. Healing of these lesions results in upper lobe volume loss with cicatricial atelectasis, architectural distortion, and traction bronchiectasis (Figs 12, 13) (5). In chronic infections, a nonspecific radiologic pattern of severe, widespread interstitial fibrosis is occasionally encountered.

Endobronchial spread is the most common complication of tuberculous cavitation and represents a chronic granulomatous infection in which active organisms spread via airways after caseous necrosis of bronchial walls. High-resolution CT is sensitive in the detection of early endobronchial spread of disease, which manifests as small, poorly defined centrilobular nodules and branching centrilobular areas of increased opacity ("tree-in-bud" appearance) representing severe bronchiolar impaction, with clubbing of distal bronchioles occurring at more than one contiguous branching site (Fig 14) (11–14). This tree-in-bud appearance is characteristic of but not pathognomonic

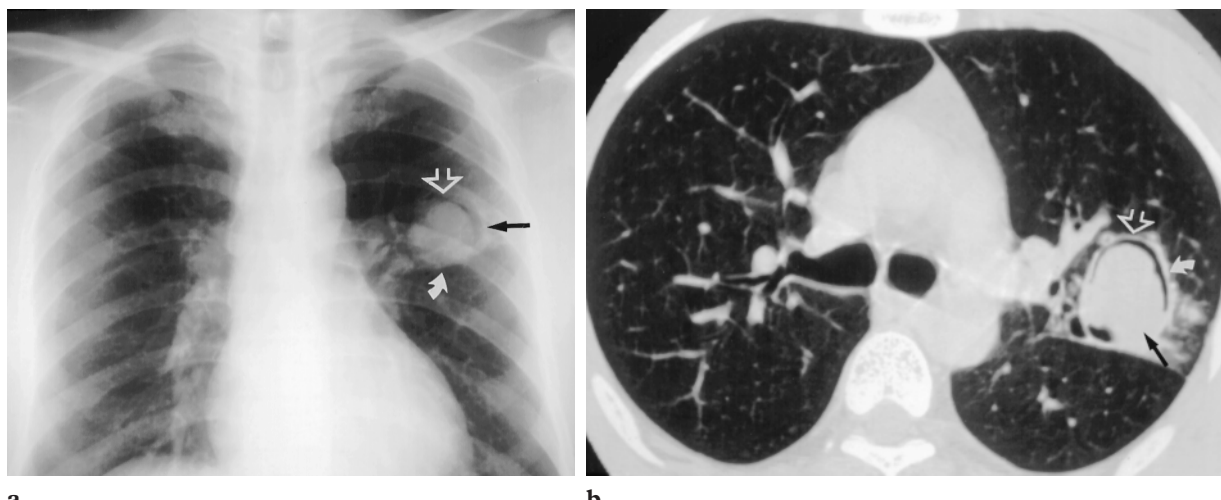
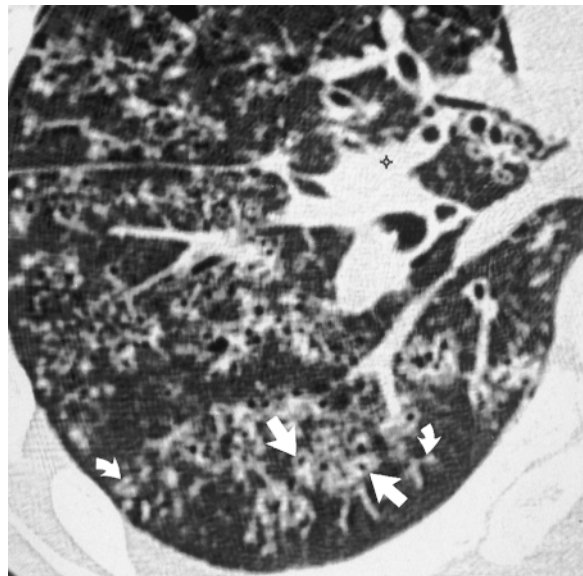


**Figure 15.** Cavitary tuberculosis associated with aspergilloma. (a) Frontal radiograph shows a cavity in the left upper lobe (black arrow) with a dependent area of soft-tissue opacity (solid white arrow). The crescentic area of hyperlucency (open arrow) represents residual air in the cavity and is referred to as the air crescent sign. (b) Axial CT scan shows dependent soft-tissue aspergilloma (black arrow) within the cavity (solid white arrow), along with the air crescent sign (open arrow).

for active tuberculosis. This appearance can also be seen with viral, fungal, and parasitic infections, allergic bronchopulmonary aspergillosis, cystic fibrosis, aspiration pneumonitis, and rare neoplasms such as laryngotracheal papillomatosis, all of which involve the small airways (14).

Cavitation may also be complicated by the development of mycetomas, which appear as mobile intracavitary masses and produce the air crescent sign (Fig 15) (9).

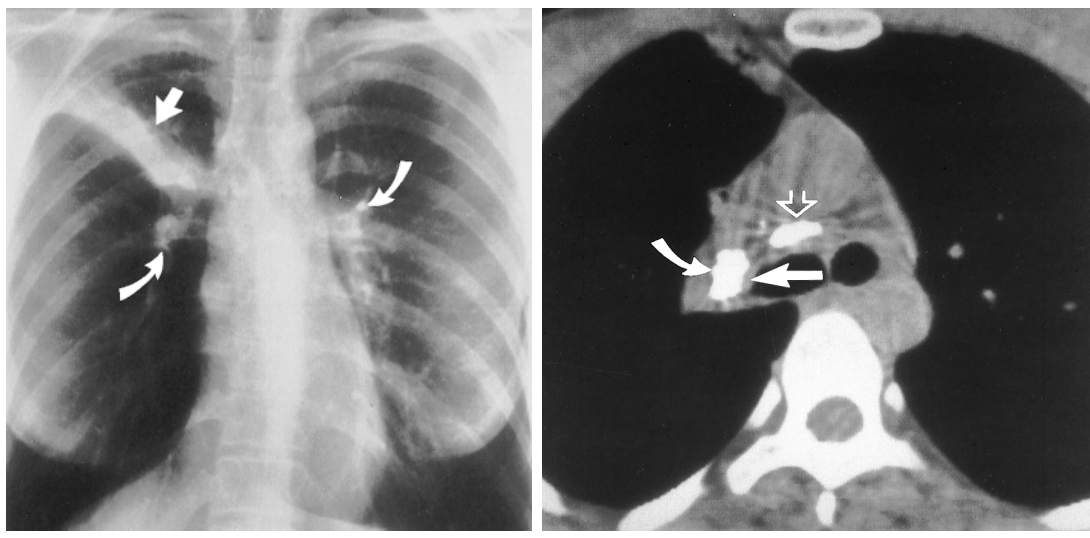
**Airway Involvement.**—Central airway involvement in tuberculosis can be the result of direct extension from tuberculous lymph nodes, endobronchial spread of infection, or lymphatic dissemination to the airway (15). Bronchial stenosis can manifest as persistent segmental or lobar collapse, lobar hyperinflation, obstructive pneumonia, or mucoid impaction. At CT, airway involvement manifests as narrowing (Fig 16) with wall thickening, complete obstruction, and obstruction due to adjoining adenopathy. These findings are nonspecific, however, and central airway tuberculosis must be differentiated from bronchogenic carcinoma affecting the central airways. Longer segments of involvement, circumferential luminal narrowing, and the absence of an intraluminal mass may allow differentiation from carcinoma. However, bronchoscopy may be required to con-



**Figure 14.** Endobronchial spread of tuberculosis. Axial CT scan shows severe changes of bronchiolar dilatation and impaction. Bronchiolar wall thickening (straight arrows) and mucoid impaction of contiguous branching bronchioles produce a tree-in-bud appearance (curved arrows).

firm the diagnosis (16). Endobronchial metastases are rare but may also appear similar to bronchial stenosis.

Calcified tuberculous lymph nodes in the mediastinum may occasionally erode into the adjacent airway (broncholithiasis) (Fig 17) (17).

**a.****b.**

**Figure 17.** Tuberculous broncholithiasis. **(a)** Chest radiograph demonstrates partial atelectasis of the right upper lobe (straight arrow) with calcified hilar lymph nodes bilaterally (curved arrows). **(b)** Axial CT scan demonstrates erosion of the right main bronchus (straight solid arrow) by a calcified hilar lymph node (curved arrow). A calcified precarinal lymph node is also noted (open arrow). The differential diagnosis for mediastinal lymph node calcification includes histoplasmosis, silicosis, and treated lymphoma.

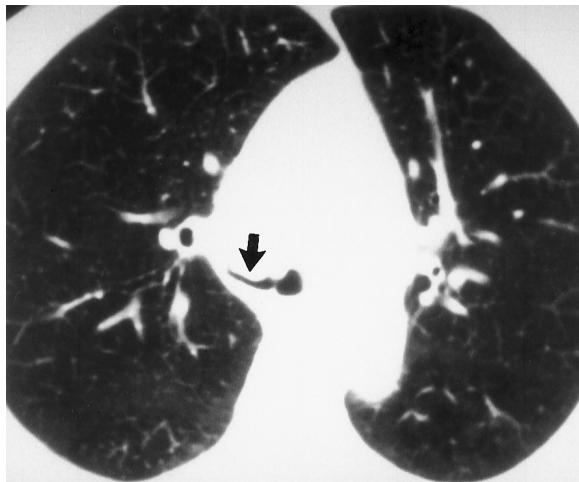


**Figure 16.** Tuberculous bronchostenosis. Axial CT scan demonstrates narrowing of the right main bronchus (arrow).

Bronchiectasis is a common complication of endobronchial tuberculosis and is typically secondary to pulmonary destruction and fibrosis (traction bronchiectasis), although it may also result from central bronchostenosis (8).

Tracheal and laryngeal tuberculosis are less common than endobronchial tuberculosis.

**Pleural Extension.**—Pleural effusions in post-primary tuberculosis are usually small and are associated with parenchymal disease. Tuberculous empyema may manifest as a loculated pleural fluid collection with parenchymal disease and cavitation. Subpleural parenchymal cavitation is seen in nearly 50% of patients with pleural tuberculosis (18). Air-fluid levels in the pleural space indicate bronchopleural fistula. Residual pleural thickening and calcification may be seen following therapy (7).

**Chest Wall Tuberculosis.**—Chest wall tuberculosis is usually secondary to pleural disease and empyema or due to hematogenous spread of disease. It is characterized by destruction of bone or costal cartilage and by soft-tissue masses that may demonstrate calcification or rim enhancement on contrast-enhanced images (Fig 18) (19,20). Fistulization to skin may also occur.

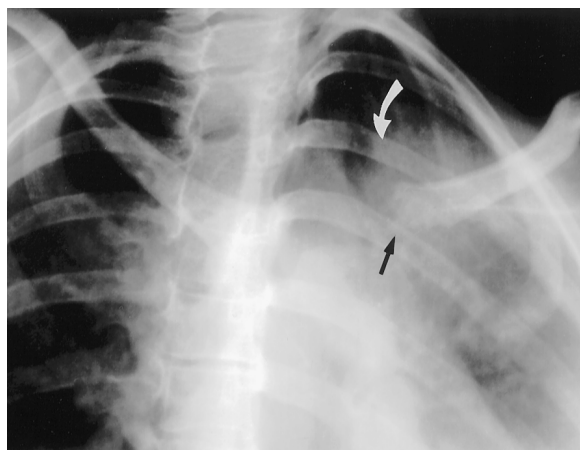


**Figure 18.** Tuberculous involvement of the left sternoclavicular joint. Oblique radiograph demonstrates irregularity of the medial end of the left clavicle (black arrow) with an associated soft-tissue mass (white arrow).

### Treatment

Plombage was a type of pulmonary collapse therapy used for treatment of tuberculosis prior to the advent of antituberculous drugs and consisted of the insertion of plastic packs, Lucite balls (Fig 19), or polythene spheres in the pleural space. Injection of oil or paraffin (oleothorax) was also performed (21,22).

### Cardiac Tuberculosis

Although tuberculosis rarely involves the heart (Fig 20), pericardial involvement may occasionally be seen with mediastinal and pulmonary tuberculosis (Fig 21) and is a cause of calcific pericarditis (23).

### Skeletal Tuberculosis

#### Tuberculous

#### Spondylitis (Pott Disease)

The spine is the most frequent site of osseous involvement in tuberculosis (24), with the upper lumbar and lower thoracic spine being involved most frequently. More than one vertebra is typically affected, and the vertebral body is more commonly involved than the posterior elements. An anterior predilection is seen in the vertebral body (25–28).

The disease process begins in the anterior part of the vertebral body adjacent to either the superior or inferior end plates (29). The infection



**Figure 19.** Plombage in a patient with postprimary tuberculosis. Frontal chest radiograph demonstrates typical right-sided Lucite ball plombage. There is thinning and disorganization of the overlying ribs (straight arrow). Air-fluid levels in the Lucite balls (curved arrows) suggest bronchopleural fistulas.

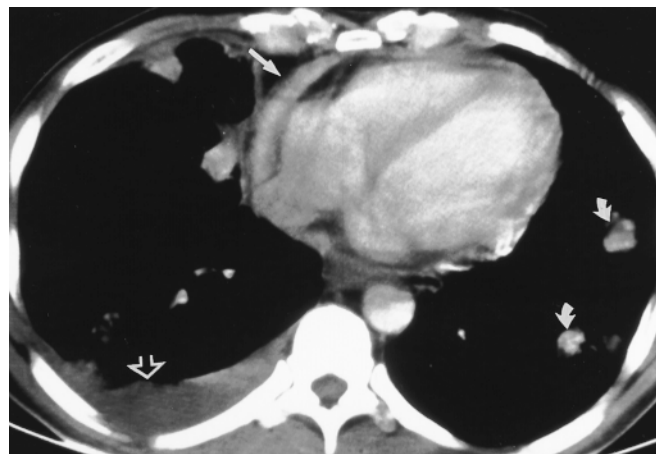
spreads to involve the adjoining disk spaces by (a) extension beneath the anterior or posterior longitudinal ligament, or (b) penetration of the subchondral bone plate (30). Involvement of the disk manifests as collapse of the intervertebral disk space (27,31,32).

Deminerelization of the end plates (Fig 22) occurs with resorption and loss of dense margins. Although a well-defined margin of destruction is usually present, reactive sclerosis or periosteal reaction in the adjoining vertebral body is typically absent. With progression of disease, there is development of progressive vertebral collapse with anterior wedging leading to the characteristic angulation and gibbus formation. Extension of tuberculosis from the vertebra and disk to adjoining ligaments and soft tissues is seen frequently and usually occurs anterolaterally. Subligamentous extension of a tuberculous abscess can be seen as erosion of the anterior surface of the vertebral bodies distant from the primary site of involvement (Fig 23) (30,31,33–39).

Paravertebral abscesses form early and are easily seen in the thoracic region as posterior mediastinal masses. Paravertebral psoas abscess in the lumbar spine can produce significant paraspinal soft-tissue opacity. The psoas abscess may extend into the groin and thigh. Occasionally, a large, paraspinal cold abscess with no osseous lesion is

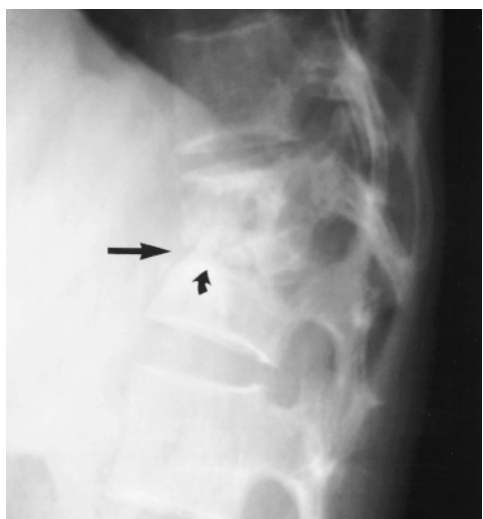


20.



21.

**Figures 20, 21.** (20) Tuberculoma of the right atrium in a patient with miliary tuberculosis. Axial T2-weighted magnetic resonance (MR) image demonstrates a hyperintense mass in the right atrium (straight arrow). Note also the right pleural effusion (curved arrow). The mass proved to be a tuberculoma at surgery. (21) Tuberculous pericarditis in a patient with pleuropulmonary tuberculosis. Axial CT scan demonstrates pericardial thickening (straight solid arrow). Pulmonary tuberculomas (curved arrows) and a right pleural effusion (open arrow) are also seen.

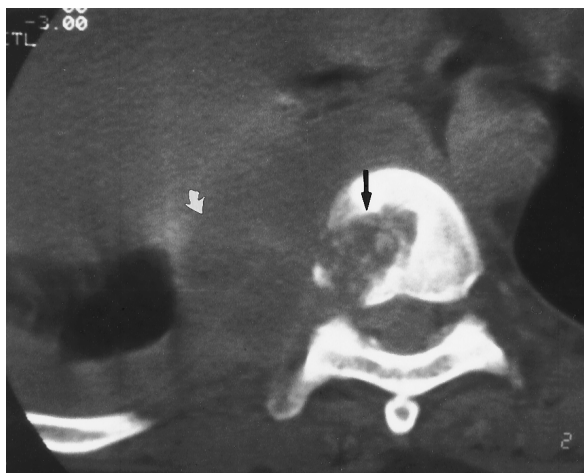


22.

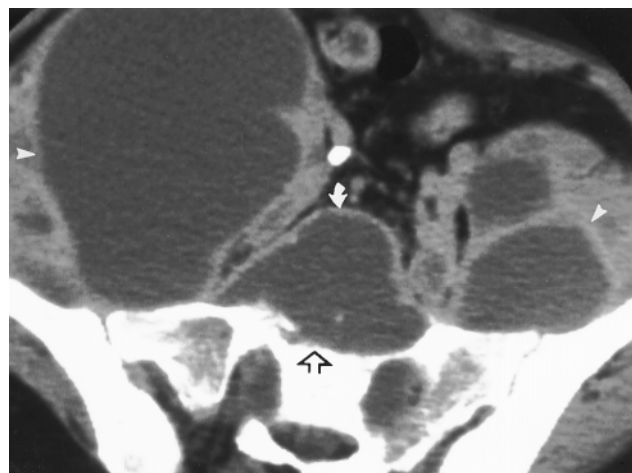


23.

**Figures 22, 23.** (22) Tuberculous spondylitis. Lateral radiograph demonstrates obliteration of the disk space (straight arrow) with destruction of the adjacent end plates (curved arrow) and anterior wedging. (23) Subligamentous spread of spinal tuberculosis. Lateral radiograph demonstrates erosion of the anterior margin of the vertebral body (arrow) caused by an adjacent soft-tissue abscess.



24.



25.

**Figures 24–26.** (24) Tuberculous spondylitis. Axial CT scan demonstrates lytic destruction of the vertebral body (black arrow) with an adjoining soft-tissue abscess (white arrow). (25) Iliopsoas abscess. Axial CT scan demonstrates large, multiloculated iliopsoas abscesses bilaterally (arrowheads). Note also the presacral abscess (solid arrow) accompanied by erosion of the anterior sacrum (open arrow). (26) Calcified psoas abscess. Axial CT scan demonstrates bilateral tuberculous psoas abscesses with peripheral calcification (arrows).

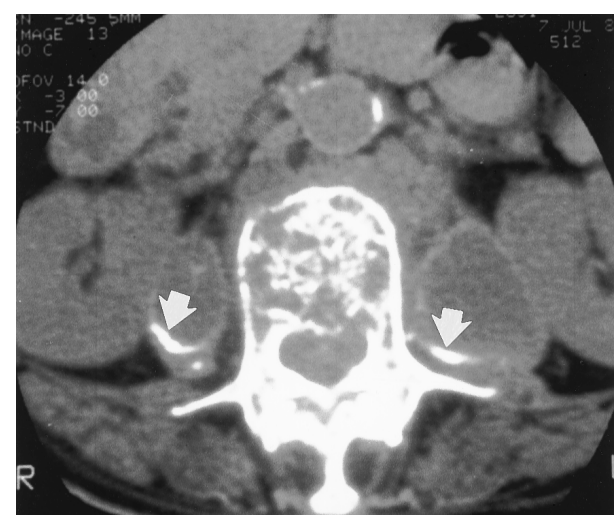
identified at radiography. In such cases, CT is of great value in demonstrating a small focus of vertebral involvement (Figs 24, 25). A healed psoas abscess may calcify (Fig 26) (39,40).

MR imaging of the spine is also useful in diagnosing tuberculous spondylitis (Fig 27) (25,28, 41,42). Typical findings include a focal area of decreased signal intensity on T1-weighted images and increased signal intensity on T2-weighted images. With involvement of the disk, increased signal intensity is noted within the disk space.

The most important differential diagnosis is pyogenic vertebral osteomyelitis. Other entities that may mimic tuberculous spondylitis include vertebral body metastases, sarcoidosis, primary vertebral neoplasm (lymphoma, multiple myeloma, chordoma), and rare spinal infections such as brucellosis, fungal disease, and echinococcosis.

### Extraspinal Tuberculous Osteomyelitis

Tuberculous osteomyelitis is usually hematogenous in origin and is most commonly seen in bones of the extremities, including the small



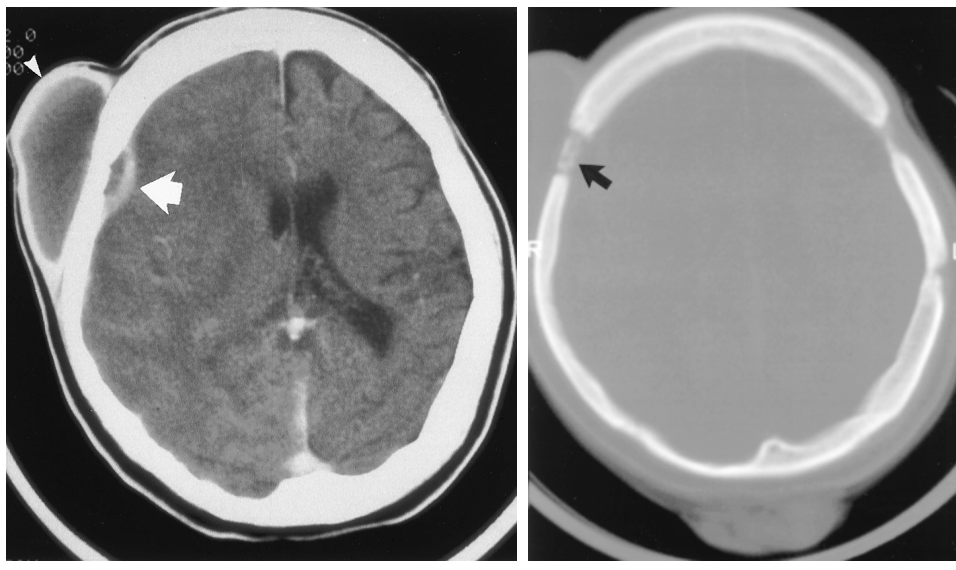
26.

bones of the hands and feet. In long, tubular bones, tuberculosis often involves the epiphyses. In children, metaphyseal foci can involve the growth plate. This feature differentiates tuberculosis from pyogenic infection (31,39).

The initial radiologic appearance of tuberculous osteomyelitis is similar to that of other types of osteomyelitis and includes foci of osteolysis with varying degrees of eburnation and periostitis (Fig 28) (39,43,44).

The diagnosis is usually made after considerable delay, and radiographic changes are seen at clinical presentation; in contrast, in pyogenic infection, radiographic changes occur 2–3 weeks after presentation.

**Cystic Tuberculosis.**—Cystic tuberculosis is a type of tuberculous osteomyelitis that affects children more often than adults. The lesions consist of



a.

b.

**Figure 28.** Tuberculous osteomyelitis involving the skull. (a) Axial contrast-enhanced CT scan demonstrates a bilobed, peripherally enhancing cold abscess centered along the right frontal bone (arrow, arrowhead). Note the significant edema and the mass effect on the underlying brain parenchyma. (b) Axial CT scan obtained with bone windowing demonstrates an ill-defined lytic area of bone destruction (arrow).



**Figure 27.** Tuberculous spondylitis. Sagittal T2-weighted MR image demonstrates areas of increased signal intensity due to edema in vertebral bodies. Accompanying disk narrowing (white arrow) and extension of the disease into the spinal canal (black arrow) are also seen.

well-defined, metaphyseal areas of hyperlucency with variable amounts of sclerosis (Fig 29) (31,45).

**Dactylitis.**—Tuberculous dactylitis involves the short tubular bones of the hands and feet in children (30). At radiography, these lesions demonstrate soft-tissue swelling and periostitis. These

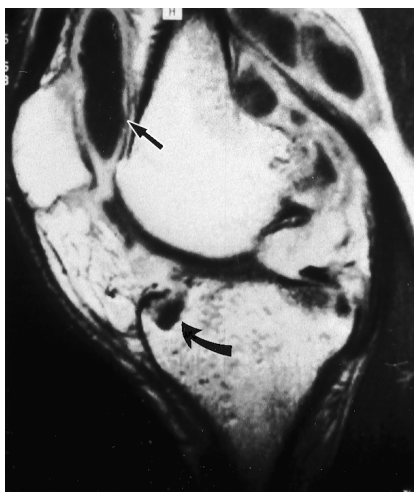


**Figure 29.** Tuberculous osteomyelitis. Anteroposterior radiograph demonstrates a lytic area of bone destruction (arrow) with transphyseal spread of infection across the growth plate.

findings are followed by gradual bone destruction and sequestrum formation. Expansion of the bone with cystic changes is known as spina ventosa (46). The radiologic differential diagnosis includes pyogenic or fungal infections, syphilitic dactylitis, sarcoidosis, hemoglobinopathies, hyperparathyroidism, and leukemia.



30.



31.



32.

**Figures 30–32.** (30) Tuberculous arthritis of the knee joint. Frontal radiograph demonstrates periarticular osteopenia (black arrow), peripheral osseous erosions (white arrow), and relative preservation of the joint space. (31) Tuberculous arthritis of the knee joint. Sagittal gadolinium-enhanced T1-weighted MR image demonstrates peripheral enhancement around the low-signal-intensity joint collection (straight arrow). Note the presence of marginal joint erosions (curved arrow). (Courtesy of Raju Sharma, MD, Department of Radiology, AIIMS, Delhi, India.) (32) Tuberculous arthritis of the ankle joint. Sagittal T1-weighted MR image demonstrates hypointense periarticular effusions (black arrows) with bone erosion of the talus and tibia (white arrow).

### Tuberculous Arthritis

Joint involvement in tuberculosis may be secondary to direct invasion from an adjacent focus of tuberculous osteomyelitis or may result from hematogenous dissemination. The disease is typically monoarticular and primarily involves the large weight-bearing joints such as the hip and knee (31,39).

A triad of radiologic abnormalities (Phemister triad) consisting of periarticular osteoporosis, peripherally located osseous erosion, and gradual diminution of the joint space suggests the diagnosis of tuberculosis (Figs 30–32) (47–51). Occasionally, wedge-shaped areas of necrosis (kissing sequestra) may be present on both sides of the affected joint. These marginal erosions may simulate rheumatoid arthritis; however, the monoarticular involvement seen in tuberculosis helps distinguish between the two conditions.

If tuberculous arthritis is left untreated, complete joint obliteration with fibrous ankylosis of the joint ensues. CT and MR imaging are helpful in the depiction of tuberculous arthritis. Other entities that may mimic this disease include pyogenic, fungal, and rheumatoid arthritis.

### Gastrointestinal Tuberculosis

Although abdominal tuberculosis is usually secondary to pulmonary tuberculosis, radiologic evaluation often shows no evidence of lung disease (52).

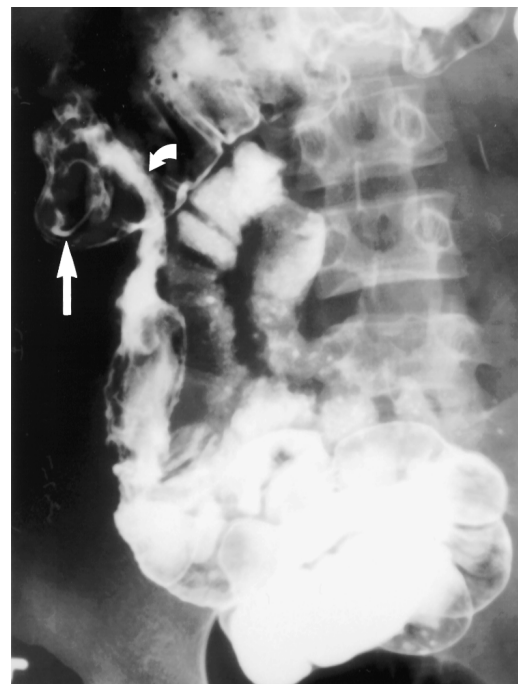
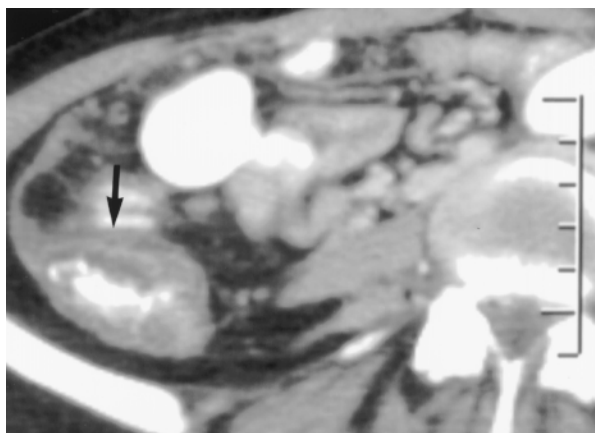


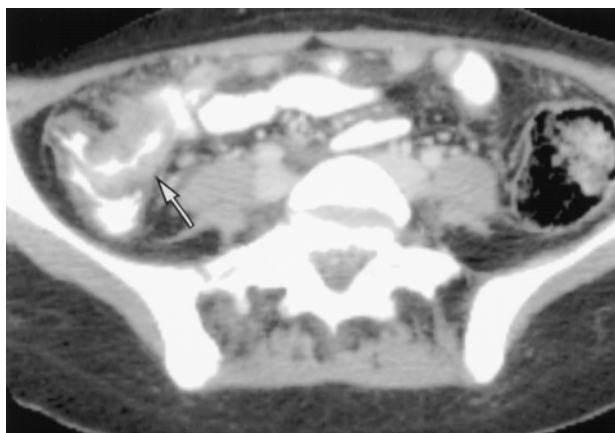
**Figure 33.** Ileocecal tuberculosis. Radiograph obtained with peroral pneumocolon technique demonstrates a conical and shrunken cecum (straight arrow) retracted out of the iliac fossa by contraction of the mesocolon. Note also the narrowing of the terminal ileum (curved arrow).

### Ileocecum and Colon

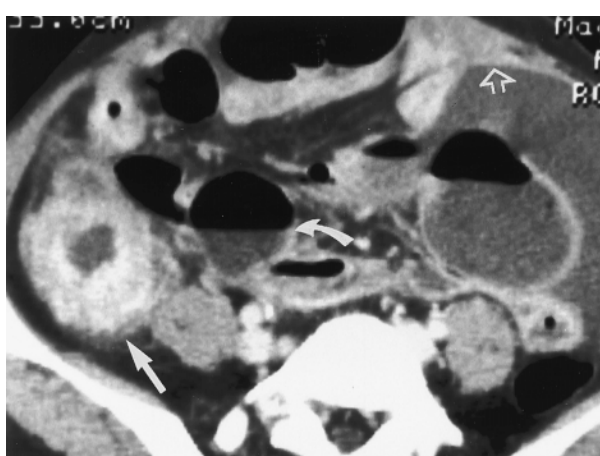
The ileocecal region is the most common area of involvement in the gastrointestinal tract due to the abundance of lymphoid tissue.



34a.



34b.



35.

The natural course of gastrointestinal tuberculosis may be ulcerative, hypertrophic, or ulcerohypertrophic (52,53).

Barium studies demonstrate spasm and hypermotility with edema of the ileocecal valve in the early stages of the disease followed by thickening of the ileocecal valve. A widely gaping ileocecal valve with narrowing of the terminal ileum (Fleischner sign) or a narrowed terminal ileum with rapid emptying of the diseased segment through a gaping ileocecal valve into a shortened, rigid, obliterated cecum (Stierlin sign) may also be seen (53). Focal or diffuse aphthous ulcers also occur in the early stages. These ulcers are larger than those seen in Crohn disease and tend to be linear or stellate, following the orientation of lymphoid follicles (ie, longitudinal in the terminal ileum and transverse in the colon) (54,55).

In advanced cases, symmetric annular stenosis and obstruction associated with shortening, retraction, and pouch formation may be seen. The cecum becomes conical, shrunken, and retracted out of the iliac fossa due to fibrosis within the

**Figures 34, 35.** (34) Ileocecal tuberculosis. (a) Axial CT scan demonstrates concentric cecal wall thickening (arrow). (b) Axial CT scan obtained caudad to a demonstrates diffuse thickening of the terminal ileum (arrow). (35) Ileocecal tuberculosis and peritoneal tuberculosis (wet type). Axial CT scan demonstrates concentric thickening of the cecum (straight solid arrow). Small bowel dilatation (curved arrow), ascites in the greater peritoneal space, and thickening of the peritoneum (open arrow) are also seen.

mesocolon, and the ileocecal valve becomes fixed, irregular, gaping, and incompetent (Fig 33) (56–58).

CT may show circumferential wall thickening of the cecum and terminal ileum associated with adjacent mesenteric lymphadenopathy (Figs 34, 35). Characteristic CT features include asymmetric thickening of the ileocecal valve and medial wall of the cecum, exophytic extension engulfing the terminal ileum, and massive lymphadenopathy (57,59,60). The lymph nodes demonstrate central areas of low attenuation.

The differential diagnosis for ileocecal tuberculosis includes amebiasis, Crohn disease, and primary cecal malignancy.

### Peritoneum

Peritoneal involvement in tuberculosis is rare and is usually associated with widespread abdominal disease involving lymph nodes or bowel (52,58). Three principal types of tuberculous peritoneal involvement are recognized. The wet type (Fig 35) is the most common and is associated with large amounts of viscous ascitic fluid that may be either diffusely distributed or loculated (58,61). The fluid demonstrates high attenuation at CT due to its high protein and cellular content (60). The dry or plastic type (Fig 36) is uncommon

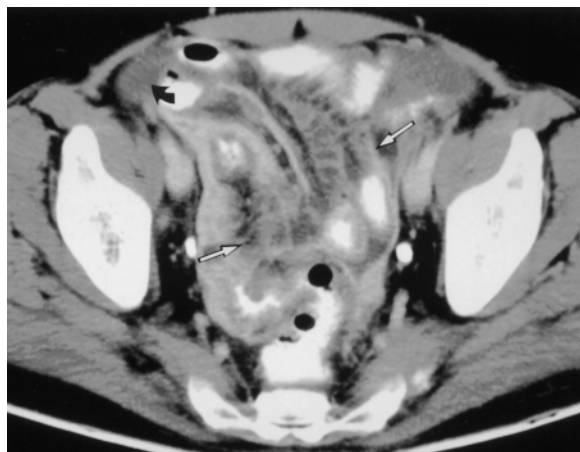


**Figure 36.** Peritoneal tuberculosis (dry type). Axial CT scan demonstrates thickening and infiltration of the peritoneum (white arrows) along with thickening of bowel loops. Note the small amount of loculated fluid (black arrow).



**Figure 37.** Peritoneal tuberculosis (fibrotic type). Axial contrast-enhanced CT scan demonstrates enhancing thickened peritoneum (straight arrow) with an adjoining matted loop of small bowel (curved arrow).

and is characterized by caseous nodules, fibrous peritoneal reaction, and dense adhesions (60,62). The fibrotic fixed type (Fig 37) consists of large omental masses, matted loops of bowel and mesentery, and, on occasion, loculated ascites (58,63). CT may also demonstrate tethering of bowel loops. Infiltration of the mesentery, when associated with a large amount of ascites, may have a stellate appearance at CT.

The radiologic differential diagnosis includes carcinomatosis, malignant mesothelioma, and nontuberculous peritonitis. Differentiation from peritoneal carcinomatosis may be difficult. Extension of the inflammation through the peritoneum into the extraperitoneal compartment suggests tuberculosis and can be helpful in differentiation.

### Lymph Nodes

Lymphadenopathy is the most common manifestation of abdominal tuberculosis (64). The mesenteric, omental, and peripancreatic lymph nodes are most commonly involved. The nodes are usually large and multiple and most commonly demonstrate peripheral enhancement with central areas of low attenuation at contrast-enhanced CT (Fig 38) (58). The radiographic appearance of tuberculosis lymphadenitis is the same in patients with and without AIDS (65).

The radiologic pattern of tuberculous lymphadenitis can also be seen with metastases, Whipple disease, lymphoma, and infection with *Mycobacterium avium-intracellulare*.



**Figure 38.** Abdominal tuberculous lymphadenitis. Axial contrast-enhanced CT scan demonstrates multiple enlarged mesenteric lymph nodes with central areas of low attenuation (arrow).

### Liver and Spleen

Tuberculosis of the liver and spleen is most likely secondary to hematogenous dissemination of the primary form of the disease.

At radiography, hepatosplenic tuberculosis may appear micronodular (miliary) or macronodular. Miliary hepatosplenic disease manifests as multiple tiny, low-attenuation foci at CT. The macronodular form is rare and manifests as diffuse liver or splenic enlargement with multiple low-attenuation lesions or a single tumorlike mass. On contrast-enhanced images, early-stage lesions may demonstrate central enhancement (Fig 39) whereas more advanced lesions may demonstrate calcification (58,66–70).

The differential diagnosis for miliary hepatosplenic tuberculosis includes metastases, fungal



**Figure 39.** Hepatic tuberculosis. Axial contrast-enhanced CT scan demonstrates multiple nonuniform, low-attenuation lesions within the liver (straight arrows). An enlarged gastrohepatic lymph node is also seen (curved arrow).

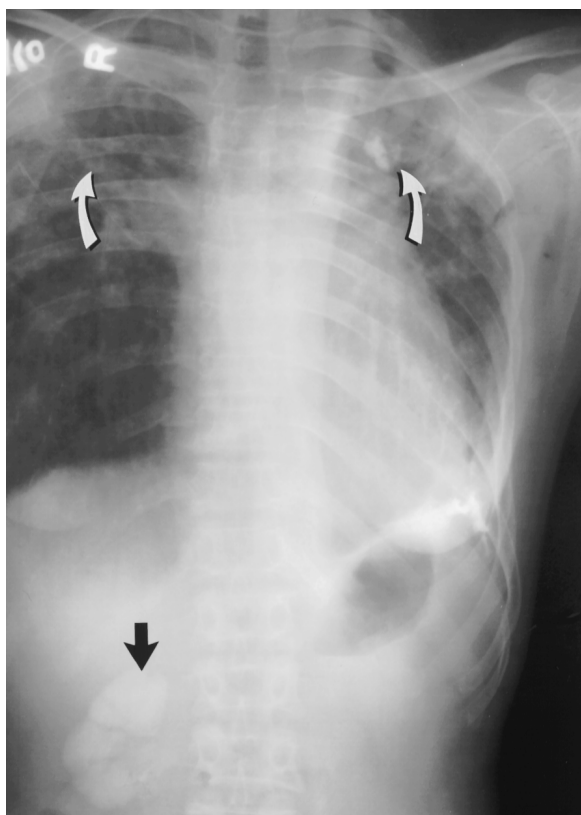


**Figure 40.** Renal tuberculosis. Chest radiograph that includes the upper abdomen demonstrates lobar calcification in the right kidney (black arrow). Note also the bilateral fibrocalcific changes in the upper lobes (white arrows).

infections, sarcoidosis, and lymphoma. The macronodular form can simulate metastases, abscess, and primary malignancy.



**Figure 41.** Tuberculous pyonephrosis. Retrograde pyelogram shows filling of the dilated hydronephrotic lower and middle pole of the right kidney. The collecting system has irregular margins (straight solid arrow) and shows irregular filling defects (curved arrow) from necrosis of the parenchyma. Upper pole calcification is also seen (open arrow).

### Genitourinary Tuberculosis

Tuberculosis may involve the genitourinary tract as a secondary site following hematogenous dissemination from the lungs.

#### Kidneys

Radiography may demonstrate calcification within the renal parenchyma. The calcification may be amorphous, granular, curvilinear, or lobar (putty kidney) (Fig 40) (71,72).

Ulceration, wall thickening, and fibrosis characterize tuberculous involvement of the collecting system. Intravenous urography demonstrates a variety of findings depending on the extent of renal involvement. The earliest urographic abnormality is a “moth-eaten” calix due to erosion. Focal or global poor renal function, dilatation of the collecting system, or irregular pools of contrast material (Fig 41) may also be seen. Infundibular stenosis may lead to incomplete opacification of the calix (phantom calix) (73). Advanced disease leads to cortical scarring with dilatation and distortion of adjoining calices, and strictures of the pelvicaliceal system produce luminal narrowing either directly or by causing kinking of the renal pelvis (Kerr kink) (53,74–76).

CT is helpful in identifying the manifestations of renal tuberculosis (Fig 42) (71,72,77) (eg,

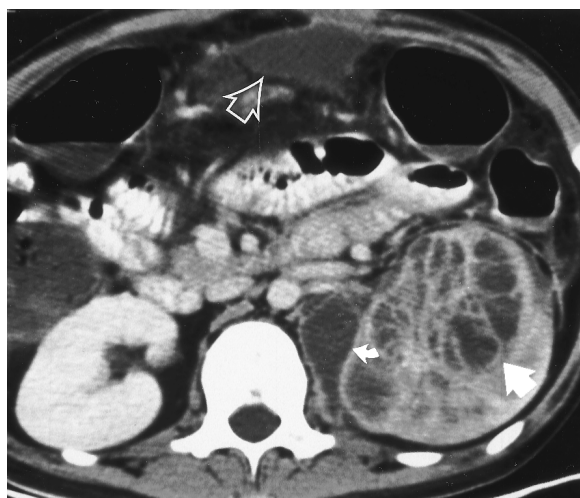


**Figure 42.** Renal tuberculosis. Axial contrast-enhanced CT scan demonstrates left tuberculous pyonephrosis (straight solid arrow) with extension of the inflammatory process into the perinephric space (curved arrow) and accompanying peritoneal disease (open arrow).

calcifications). Various patterns of hydronephrosis may be seen at CT depending on the site of the stricture and include focal caliectasis, caliectasis without pelvic dilatation, and generalized hydronephrosis (72). Other common findings include parenchymal scarring and low-attenuation parenchymal lesions. CT is also useful in depicting the extension of disease into the extrarenal space.

The radiologic differential diagnosis for renal tuberculosis includes other causes of papillary necrosis, transitional cell carcinoma, and other infections.

### Adrenal Glands

Adrenal involvement in tuberculosis is rare. It may manifest as unilateral or bilateral adrenal masses with central areas of necrosis (Fig 43). Enlarged adrenal glands are also seen in patients with recent or concurrent renal tuberculous infection (53,78–80). Adrenal atrophy with calcification may be seen in patients with healed prior tuberculosis, and these patients may present with Addison disease (81).

The radiologic differential diagnosis includes metastases, primary adrenal neoplasm, and adrenal hemorrhage.

### Ureter

Ureteral involvement is seen in 50% of patients with genitourinary tuberculosis (53). Dilatation and a ragged appearance of the ureter are usually the initial signs of ureteral tuberculosis at urography. Occasionally, filling defects due to mucosal

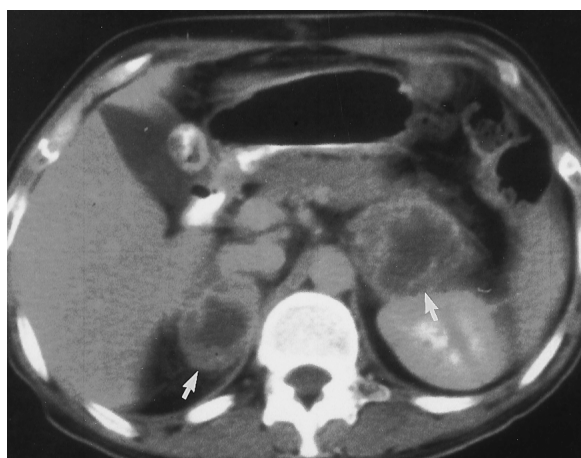


**Figure 43.** Adrenal tuberculosis. Axial contrast-enhanced CT scan demonstrates bilateral adrenal masses with central low-attenuation areas (arrows).

granulomas may be seen (74). CT may demonstrate thickening of the ureteral wall and periureteral inflammatory changes (72,77). As the disease progresses, urography demonstrates short- or long-segment ulceration of the ureter. Chronic fibrotic strictures result in a beaded or corkscrew appearance. Chronic thickening of the ureteral wall may also cause foreshortening (piping-stem ureter) (82). Wall calcifications are an infrequent finding in ureteral tuberculosis.

Ureteral tuberculosis must be differentiated from ureteral stones and calcifications caused by schistosomiasis.

### Bladder

The most common finding in tuberculous cystitis is reduced bladder capacity (53). Typically, tuberculous cystitis manifests as a shrunken bladder with wall thickening (74). Occasionally, filling defects due to multiple granulomas may also be seen. In advanced disease, the bladder may be diminutive and irregular (thimble bladder) (Figs 44, 45). Advanced bladder involvement may be complicated by vesicoureteral reflux due to fibrosis involving the ureteral orifice. Calcification of the bladder wall is rarely seen.

The radiologic differential diagnosis for tuberculous bladder calcification includes schistosomiasis, cytoxan cystitis, radiation-induced bladder calcification, calcified bladder carcinoma, and encrusted foreign materials. Bladder tuberculomas may mimic transitional cell carcinoma.

### Genitalia

Genital tuberculosis affects both males and females. Diagnostic criteria for female genital tuberculosis include endometrial adhesions with deformity and obliteration of the endometrial



44.



45.

**Figures 44, 45.** Bladder tuberculosis. (44) Axial contrast-enhanced CT scan demonstrates a thickened and deformed bladder with an enhancing wall (straight arrow). There is extension of the inflammatory process to the anterior abdominal wall (curved arrow). (45) Intravenous urogram demonstrates a thickened, contracted, low-capacity bladder (thimble bladder) (arrowhead) with minimal dilatation of both ureters.

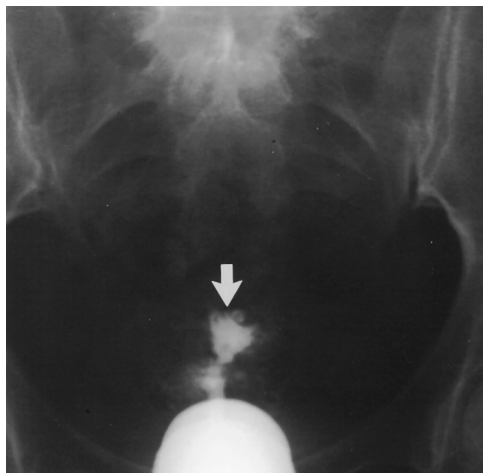


**Figure 46.** Endometrial tuberculosis. Hysterosalpingogram demonstrates an obliterated and deformed endometrial cavity (arrow) due to tuberculous endometritis.

cavity (Fig 46), obstruction of the fallopian tubes with multiple areas of constriction, and calcified lymph nodes in the adnexal region (53). Advanced tuberculous endometritis may mimic severe uterine adhesions as seen in Asherman syndrome.

In males, tuberculous involvement of the prostate gland or seminal vesicles may lead to necrosis, calcification, caseation, and cavitation (72,83, 84). Tuberculous epididymo-orchitis usually manifests at ultrasonography as focal or diffuse areas of decreased echogenicity with epididymal involvement (85).

### Tuberculosis Involving the Central Nervous System

Most tuberculous infections of the central nervous system are a result of hematogenous spread. Intracranial tuberculosis results in two related pathologic processes: tuberculous meningitis and intracranial tuberculomas. Tuberculous meningitis is a more frequent manifestation of neurotuberculosis than is brain tuberculoma and is more commonly seen in children.

#### Meningeal Involvement

Meningeal involvement is iso- or hyperattenuating relative to the basal cisterns at unenhanced CT and demonstrates intense, often homogeneous enhancement after contrast material administration. This enhancement extends into hemispheric fissures and over the cortical surfaces of the brain. Sequelae of meningeal involvement include hydrocephalus and infarcts in the middle cerebral artery distribution due to panarteritis of the vessels in the basal cisterns (86–94).

MR imaging findings vary depending on the stage of the disease. In the early stages, findings at unenhanced spin-echo imaging may be normal. In later stages, there is distention of the affected subarachnoid spaces associated with mild shortening of T1 and T2 relaxation times compared

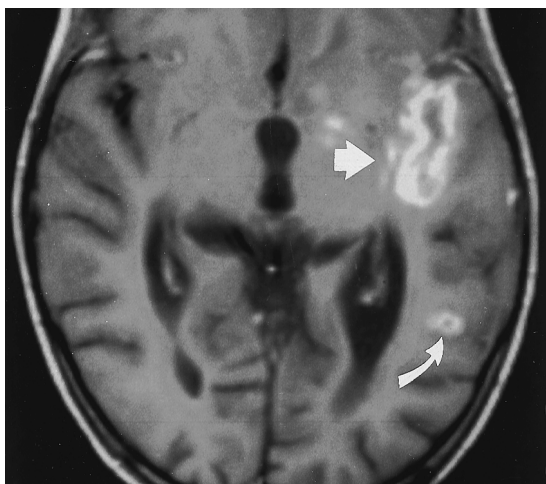


**Figure 47.** Cranial tuberculous meningitis. Axial gadolinium-enhanced T1-weighted MR image demonstrates leptomeningeal enhancement along the left sylvian fissure (straight arrow). There is an accompanying ring-enhancing granuloma in the left parieto-occipital region (curved arrow).



**Figure 48.** Cranial tuberculomas. Axial contrast-enhanced CT scan demonstrates multiple ring-enhancing lesions (straight arrows) along with diffuse meningeal enhancement (curved arrow).

with normal cerebrospinal fluid. Gadolinium-enhanced T1-weighted imaging demonstrates abnormal meningeal enhancement that is more pronounced in the basal cisterns (Fig 47). There may be involvement of the meninges within the sulci over the cerebral convexities and in the sylvian fissures. Abnormal enhancement of the choroid plexus and ependymal lining of the ventricular system may rarely be seen. Sequelae of tuberculous meningitis include focal areas of atrophy secondary to infarcts and hydrocephalus and, rarely, syringomyelia or syringobulbia (87,88,94–100).

The differential diagnosis for tuberculous meningitis includes other infectious agents (non-tuberculous bacteria, viruses, fungi, parasites), noninfectious inflammatory disease affecting the leptomeninges (rheumatoid disease, sarcoidosis), and primary or secondary neoplastic involvement of meningeal surfaces (meningiomatosis, neoplastic meningitis from a peripheral tumor source, cerebrospinal fluid seeding from a primary tumor of the central nervous system).

### Parenchymal Involvement

Parenchymal disease can occur with or without meningitis and usually manifests as either solitary or multiple tuberculomas.

At CT, tuberculomas manifest as low- or high-attenuation rounded or lobulated masses that commonly demonstrate ring enhancement on contrast-enhanced images. These lesions are often associated with moderate to marked edema (Fig 48), but calcification is uncommon (88,90,94,101,102).

MR imaging findings vary depending on whether the granulomas are noncaseating, caseating with a solid center, or caseating with a necrotic center. Tuberculomas consisting of non-caseating granulomas are usually hypointense relative to the brain on T1-weighted images and hyperintense on T2-weighted images. The lesions usually demonstrate homogeneous enhancement after gadolinium administration. Caseating granulomatous lesions with a solid center appear relatively hypointense or isointense on T1-weighted images and iso- to hypointense on T2-weighted images (Figs 49, 50). They are typically associated with surrounding edema. The lesion has a hypointense rim on T2-weighted images. Caseating lesions demonstrate rim enhancement at contrast-enhanced T1-weighted MR imaging.

Tuberculomas with a necrotic center demonstrate central hyperintensity on T2-weighted images (87,88,95,96,98,100,103–106).

The differential diagnosis for parenchymal tuberculomas includes other granulomatous infections (eg, cysticercosis) and fungal lesions as well as primary or metastatic neoplasms.

### Tuberculous Otomastoiditis

Tuberculous otomastoiditis can result from hematogenous spread or from direct extension from the upper respiratory tract (107).

CT demonstrates soft-tissue attenuation in the tympanic cavity in the early stages and destruction of middle ear structures in the later stages. Associated retroauricular or epidural abscess may also be seen (Fig 51).



49.



50.

**Figures 49, 50.** (49) Solid caseating tuberculous granulomas involving the cerebellum. Axial T2-weighted MR image demonstrates multiple granulomas with central areas of hypointensity in the cerebellum (arrows). (50) Tuberculous granulomas involving the cerebellum. Axial T1-weighted MR image demonstrates isointense lesions with mildly hyperintense rims in the cerebellum (arrows).



**Figure 51.** Bilateral tuberculous mastoiditis. High-resolution CT scan of the temporal bone demonstrates bilateral destructive lesions in the mastoid processes (straight arrows). There is an accompanying cold abscess overlying the right temporo-occipital region (curved arrow).

The differential diagnosis for tuberculous otomastoiditis includes pyogenic or fungal infection, sarcoidosis, cholesteatoma, and Wegener granulomatosis.

### Ocular Tuberculosis

Ocular tuberculosis results from hematogenous spread and can involve any part of the eye. Chorioretinitis and uveitis are the most common manifestations (107,108).

At CT or MR imaging, ocular tuberculosis usually manifests as a unilateral choroidal mass (Fig 52).

The differential diagnosis for ocular tuberculosis includes melanoma, metastasis, hemangioma, sarcoidosis, and systemic mycoses.



**Figure 52.** Orbital tuberculosis. Axial contrast-enhanced CT scan demonstrates an enhancing retinal lesion in the left orbit (arrow).

### Conclusions

Tuberculosis can affect virtually any organ system in the body and can be devastating if left untreated. The increasing prevalence of this disease in both immunocompetent and immunocompromised individuals makes tuberculosis a topic of universal concern. Tuberculosis has a variety of radiologic appearances and can mimic numerous other disease entities. A high degree of clinical suspicion and familiarity with the various radiologic manifestations of tuberculosis allow early diagnosis and timely initiation of appropriate therapy, thereby reducing patient morbidity.

## References

1. Davis SD, Yankelevitz DF, Williams T, et al. Pulmonary tuberculosis in immunocompromised hosts: epidemiological, clinical, and radiological assessment. *Semin Roentgenol* 1993; 28:119-130.
2. Woodring JH, Vandiviere HM, Fried AM, et al. Update: the radiographic features of pulmonary tuberculosis. *AJR Am J Roentgenol* 1986; 146: 497-506.
3. McAdams HP, Erasmus J, Winter JA. Radiologic manifestations of pulmonary tuberculosis. *Radiol Clin North Am* 1995; 33:655-678.
4. Miller WT, Miller WT Jr. Tuberculosis in the normal host: radiological findings. *Semin Roentgenol* 1993; 28:109-118.
5. Palmer PE. Pulmonary tuberculosis: usual and unusual radiographic presentations. *Semin Roentgenol* 1979; 14:204-243.
6. Hong SH, Im JG, Lee JS, et al. High resolution CT findings of miliary tuberculosis. *J Comput Assist Tomogr* 1998; 22:220-224.
7. Lee KS, Im JG. CT in adults with tuberculosis of the chest: characteristic findings and role in management. *AJR Am J Roentgenol* 1995; 164: 1361-1367.
8. Im JG, Itoh H, Han MC. CT of pulmonary tuberculosis. *Semin Ultrasound CT MR* 1995; 16: 420-434.
9. Kuhlman JE, Deutsch JH, Fishman EK, et al. CT features of thoracic mycobacterial disease. *RadioGraphics* 1990; 10:413-431.
10. Makanjuola D. Fluid levels in pulmonary tuberculosis cavities in a rural population of Nigeria. *AJR Am J Roentgenol* 1983; 141:519-520.
11. Im JG, Itoh H, Shim YS, et al. Pulmonary tuberculosis: CT findings—early active disease and sequential change with antituberculous therapy. *Radiology* 1993; 186:653-660.
12. Calpe JL, Chiner E, Laramendi CH. Endobronchial tuberculosis in HIV-infected patients. *AIDS* 1995; 9:1159-1164.
13. Lee KS, Kim YH, Kim WS, et al. Endobronchial tuberculosis: CT features. *J Comput Assist Tomogr* 1991; 15:424-428.
14. Collins J, Blankenbaker D, Stern E. CT patterns of bronchiolar disease: what is tree-in-bud? *AJR Am J Roentgenol* 1998; 171:365-370.
15. Smith LS, Schillaci RF, Sarlin RF. Endobronchial tuberculosis: serial fiberoptic bronchoscopy and natural history. *Chest* 1987; 91:644-647.
16. Moon WK, Im JG, Yeon KM, et al. Tuberculosis of the central airways: CT findings of active and fibrotic disease. *AJR Am J Roentgenol* 1997; 169:649-653.
17. Vix V. Radiographic manifestations of broncholithiasis. *Radiology* 1978; 128:295-299.
18. Hulnick D, Naidich D, McCauley D. Pleural tuberculosis evaluated by computed tomography. *Radiology* 1983; 149:759-765.
19. Adler BD, Padley SP, Mü NL. Tuberculosis of the chest wall: CT findings. *J Comput Assist Tomogr* 1993; 17:271-273.
20. Lee G, Im JG, Kim JS, et al. Tuberculosis of the ribs: CT appearance. *J Comput Assist Tomogr* 1993; 17:363-366.
21. Winer-Muram H, Rubin S. Thoracic complications of tuberculosis. *J Thorac Imaging* 1990; 5: 46-63.
22. Shepard M. Plombage in the 1980s. *Thorax* 1985; 40:328-340.
23. Taillefer R, Lemieux RJ, Picard D, et al. Gallium-67 imaging in pericarditis secondary to tuberculosis and histoplasmosis. *Clin Nucl Med* 1981; 6:413-415.
24. Martini M, Quahes M. Bone and joint tuberculosis: a review of 652 cases. *Orthopedics* 1988; 2: 861-866.
25. Ahmadi J, Bajaj A, Destian S, et al. Spinal tuberculosis: atypical observations at MR imaging. *Radiology* 1993; 189:489-493.
26. Azzam NI, Tammawy M. Tuberculous spondylitis in adults: diagnosis and treatment. *Br J Neurosurg* 1988; 2:85-91.
27. Boxer DL, Pratt C, Hine AL, et al. Radiological features during and following treatment of spinal tuberculosis. *Br J Radiol* 1992; 65:476-479.
28. al-Mulhim FA, Ibrahim EM, el-Hassan AY, et al. Magnetic resonance imaging of tuberculous spondylitis. *Spine* 1995; 20:2287-2292.
29. Weaver P, Lifeso R. The radiological diagnosis of tuberculosis of the adult spine. *Skeletal Radiol* 1984; 12:178-186.
30. Chapman M, Murray R, Stocker D. Tuberculosis of the bones and joints. *Semin Roentgenol* 1979; 14:266-282.
31. Resnik D, Niwayama G. Diagnoses of bone and joint disorders. Vol 4. Philadelphia, Pa: Saunders, 1988.
32. Desai SS. Early diagnosis of spinal tuberculosis by MRI. *J Bone Joint Surg Br* 1994; 76:863-869.
33. Ehara S, Shimamura T, Wada T. Single vertebral compression and involvement of the posterior elements in tuberculous spondylitis: observation on MR imaging. *Radiat Med* 1997; 15:143-147.
34. al Arabi KM, al Sebai MW, al Chakaki M. Evaluation of radiological investigations in spinal tuberculosis. *Int Orthop* 1992; 16:165-167.
35. Hoffman EB, Crosier JH, Cremin BJ. Imaging in children with spinal tuberculosis: a comparison of radiography, computed tomography and magnetic resonance imaging. *J Bone Joint Surg Br* 1993; 75:233-239.
36. Rathakrishnan V, Mohd TH. Osteo-articular tuberculosis: a radiological study in a Malaysian hospital. *Skeletal Radiol* 1989; 18:267-272.
37. Shanley DJ. Tuberculosis of the spine: imaging features. *AJR Am J Roentgenol* 1995; 164:659-664.
38. Sharif HS, Clark DC, Aabed MY, et al. Granulomatous spinal infections: MR imaging. *Radiology* 1990; 177:101-107.
39. Yao D, Sartoris D. Musculoskeletal tuberculosis. *Radiol Clin North Am* 1995; 33:679-689.
40. Lindahl S, Nyman RS, Brismar J, et al. Imaging of tuberculosis. IV. Spinal manifestations in 63 patients. *Acta Radiol* 1996; 37:506-511.
41. Arizona T, Oga M, Shiota E, et al. Differentiation of vertebral osteomyelitis and tuberculous spondylitis by magnetic resonance imaging. *Int Orthop* 1995; 19:319-322.

42. Smith AS, Weinstein MA, Mizushima A, et al. MR imaging characteristics of tuberculous spondylitis vs vertebral osteomyelitis. *AJR Am J Roentgenol* 1989; 153:399–405.
43. Barrington NA. The radiology of bone and joint infection. *Br J Hosp Med* 1988; 40:464–472.
44. Muradali D, Gold WL, Vellend H, et al. Multi-focal osteoarticular tuberculosis: report of four cases and review of management. *Clin Infect Dis* 1993; 17:204–209.
45. Rasool M, Govender S, Naidoo K. Cystic tuberculosis of bone in children. *J Bone Joint Surg Br* 1994; 76:113–117.
46. Feldman F, Auerbach R, Hohnston A. Tuberculous dactylitis in the adult. *Am J Roentgenol Rad Ther* 1971; 112:460–479.
47. Campbell JA, Hoffman EB. Tuberculosis of the hip in children. *J Bone Joint Surg Br* 1995; 77: 319–326.
48. Dhillon MS, Sharma S, Gill SS, et al. Tuberculosis of bones and joints of the foot: an analysis of 22 cases. *Foot Ankle* 1993; 14:505–513.
49. Hugosson C, Nyman RS, Brismar J, et al. Imaging of tuberculosis. V. Peripheral osteoarticular and soft-tissue tuberculosis. *Acta Radiol* 1996; 37:512–516.
50. Lee AS, Campbell JA, Hoffman EB. Tuberculosis of the knee in children. *J Bone Joint Surg Br* 1995; 77:313–318.
51. Suh JS, Lee JD, Cho JH, et al. MR imaging of tuberculous arthritis: clinical and experimental studies. *J Magn Reson Imaging* 1996; 6:185–189.
52. Jadavar H, Mindelzun R, Olcott E, et al. Still the great mimicker: abdominal tuberculosis. *AJR Am J Roentgenol* 1997; 168:1455–1460.
53. Leder RA, Low VH. Tuberculosis of the abdomen. *Radiol Clin North Am* 1995; 33:691–705.
54. Thoeni R, Margulis A. Gastrointestinal tuberculosis. *Semin Roentgenol* 1979; 14:283–294.
55. Nakano H, Jaramillo E, Watanabe M, et al. Intestinal tuberculosis: findings on double contrast barium enema. *Gastrointest Radiol* 1992; 17: 108–114.
56. Healy JC, Gorman S, Kumar PJ. Tuberculous colitis mimicking Crohn's disease: case report. *Clin Radiol* 1992; 46:131–132.
57. Bargallo N, Nicolau C, Luburich P, et al. Intestinal tuberculosis in AIDS. *Gastrointest Radiol* 1992; 17:115–118.
58. Denton T, Hossain J. A radiological study of abdominal tuberculosis in a Saudi population, with special reference to ultrasound and computed tomography. *Clin Radiol* 1993; 47:409–414.
59. Balthazar EJ, Gordon R, Hulnick D. Ileocecal tuberculosis: CT and radiologic evaluation. *AJR Am J Roentgenol* 1990; 154:499–503.
60. Denath FM. Abdominal tuberculosis in children: CT findings. *Gastrointest Radiol* 1990; 15:303–306.
61. Lee DH, Lim JH, Ko YT, et al. Sonographic findings in tuberculous peritonitis of wet-ascitic type. *Clin Radiol* 1991; 44:306–310.
62. Ramaiya LI, Walter DF. Sonographic features of tuberculous peritonitis. *Abdom Imaging* 1993; 18:23–26.
63. Zirinsky K, Auh YH, Kneeland JB, et al. Computed tomography, sonography, and MR imaging of abdominal tuberculosis. *J Comput Assist Tomogr* 1985; 9:961–963.
64. Hulnick D, Megibow A, Naidich D, et al. Abdominal tuberculosis: CT evaluation. *Radiology* 1985; 157:199–204.
65. Radin DR. Intraabdominal *Mycobacterium tuberculosis* vs *Mycobacterium avium-intracellulare* infections in patients with AIDS: distinction based on CT findings. *AJR Am J Roentgenol* 1991; 156:487–491.
66. Choi BI, Im JG, Han MC, et al. Hepatosplenic tuberculosis with hypersplenism: CT evaluation. *Gastrointest Radiol* 1989; 14:265–267.
67. Malde HM, Chadha D. The “cluster” sign in macronodular hepatic tuberculosis: CT features. *J Comput Assist Tomogr* 1993; 17:159–161.
68. Buxi TB, Vohra RB, Sujatha Y, et al. CT appearances in macronodular hepatosplenic tuberculosis: a review with five additional new cases. *Comput Med Imaging Graph* 1992; 16:381–387.
69. Levine C. Primary macronodular hepatic tuberculosis: US and CT appearances. *Gastrointest Radiol* 1990; 15:307–309.
70. Nampoory MR, Halim MM, Sreedharan R, et al. Liver abscess and disseminated intravascular coagulation in tuberculosis. *Postgrad Med J* 1995; 71:490–492.
71. Premkumar A, Lattimer J, Newhouse JH. CT and sonography of advanced urinary tract tuberculosis. *AJR Am J Roentgenol* 1987; 148:65–69.
72. Wang LJ, Wong YC, Chen CJ, et al. CT features of genitourinary tuberculosis. *J Comput Assist Tomogr* 1997; 21:254–258.
73. Brennan RE, Pollack HM. Nonvisualized (“phantom”) renal calyx: causes and radiological approach to diagnosis. *Urol Radiol* 1979; 1:17–23.
74. Roylance J, Penry JB, Davies ER, et al. The radiology of tuberculosis of the urinary tract. *Clin Radiol* 1970; 21:163–170.
75. Roylance J, Penry JB, Davies ER, et al. Radiology in the management of urinary tract tuberculosis. *Br J Urol* 1970; 42:679–687.
76. Skutil V, Gow JG. Urogenital tuberculosis: the present state in Europe—the report of round table discussion. *Eur Urol* 1977; 3:257.
77. Goldman S, Fishman E, Hartman D, et al. Computed tomography of renal tuberculosis and its pathological correlates. *J Comput Assist Tomogr* 1985; 9:771–776.
78. Buxi TB, Vohra RB, Sujatha Y, et al. CT in adrenal enlargement due to tuberculosis: a review of literature with five new cases. *Clin Imaging* 1992; 16:102–108.
79. Hauser H, Gurret JP. Miliary tuberculosis associated with adrenal enlargement: CT appearance. *J Comput Assist Tomogr* 1986; 10:254–256.
80. Penne D, Oyen R, Demedts M, et al. Tuberculosis of the adrenal glands: diagnosis by CT-guided fine needle biopsy. *J Belge Radiol* 1993; 76:324–325.

81. Sawczuk IS, Reitelman C, Libby C, et al. CT findings in Addison's disease caused by tuberculosis. *Urol Radiol* 1986; 8:44–45.
82. Birnbaum BA, Friedman JP, Lubat E, et al. Extrarenal genitourinary tuberculosis: CT appearance of calcified pipe-stem ureter and seminal vesicle abscess. *J Comput Assist Tomogr* 1990; 14:653–655.
83. Premkumar A, Newhouse JH. Seminal vesicle tuberculosis: CT appearance. *J Comput Assist Tomogr* 1988; 12:676–677.
84. Wang JH, Chang T. Tuberculosis of the prostate: CT appearance. *J Comput Assist Tomogr* 1991; 15:269–270.
85. Heaton ND, Hogan B, Michell M, et al. Tuberculous epididymo-orchitis: clinical and ultrasound observations. *Br J Urol* 1989; 64:305–309.
86. Goyal M, Sharma A, Mishra NK, et al. Imaging appearance of pachymeningeal tuberculosis. *AJR Am J Roentgenol* 1997; 169:1421–1424.
87. Jamieson DH. Imaging intracranial tuberculosis in childhood. *Pediatr Radiol* 1995; 25:165–170.
88. Villoria MF, Fortea F, Moreno S, et al. MR imaging and CT of central nervous system tuberculosis in the patient with AIDS. *Radiol Clin North Am* 1995; 33:805–820.
89. Wallace RC, Burton EM, Barrett FF, et al. Intracranial tuberculosis in children: CT appearance and clinical outcome. *Pediatr Radiol* 1991; 21:241–246.
90. de Castro CC, de Barros NG, Campos ZM, et al. CT scans of cranial tuberculosis. *Radiol Clin North Am* 1995; 33:753–769.
91. Shanley DJ. Computed tomography and magnetic resonance imaging of tuberculous meningitis. *J Am Osteopath Assoc* 1993; 93:497–501.
92. De Volder I, Truyen L, Van Goethem J, et al. Tuberculous meningitis in immunocompetent adults: two cases with a clinico-radiological discussion. *Clin Neurol Neurosurg* 1996; 98:312–317.
93. Jinkins JR. Computed tomography of intracranial tuberculosis. *Neuroradiology* 1991; 33:126–135.
94. Bahemuka M, Murungi JH. Tuberculosis of the nervous system: a clinical, radiological and pathological study of 39 consecutive cases in Riyadh, Saudi Arabia. *J Neurol Sci* 1989; 90:67–76.
95. Just M, Higer HP, Krämer G, et al. Magnetic resonance imaging in infections of the brain: findings in tuberculosis, listeriosis, toxoplasmosis, subacute sclerosing panencephalitis, and multiple sclerosis. *Neurosurg Rev* 1987; 10:185–190.
96. Jinkins JR, Gupta R, Chang KH, et al. MR imaging of central nervous system tuberculosis. *Radiol Clin North Am* 1995; 33:771–786.
97. Brismar J, Hugosson C, Larsson SG, et al. Imaging of tuberculosis. III. Tuberculosis as a mimicker of brain tumour. *Acta Radiol* 1996; 37:496–505.
98. Just M, Higer HP, Betting O, et al. MRI in cranial tuberculosis. *Eur J Radiol* 1987; 7:276–278.
99. Davidson HD, Steiner RE. Magnetic resonance imaging in infections of the central nervous system. *AJNR Am J Neuroradiol* 1985; 6:499–504.
100. Kioumehr F, Dadsetan MR, Rooholamini SA, et al. Central nervous system tuberculosis: MRI. *Neuroradiology* 1994; 36:93–96.
101. Seow WT, Yeo TT, Ong PL. Tuberculoma of the brain: report of 2 cases and review of literature. *Singapore Med J* 1991; 32:427–430.
102. Dao DA, Lee PW, Roy TM. Intracranial tuberculoma. *J Ky Med Assoc* 1990; 88:121–124.
103. Gupta RK, Gupta S, Singh D, et al. MR imaging and angiography in tuberculous meningitis. *Neuroradiology* 1994; 36:87–92.
104. Chang KH, Han MH, Roh JK, et al. Gd-DTPA enhanced MR imaging in intracranial tuberculosis. *Neuroradiology* 1990; 32:19–25.
105. Gupta RK, Jena A, Sharma A, et al. MR imaging of intracranial tuberculomas. *J Comput Assist Tomogr* 1988; 12:280–285.
106. Salgado P, Del Brutto OH, Talamas O, et al. Intracranial tuberculoma: MR imaging. *Neuroradiology* 1989; 31:299–302.
107. Moon WK, Han MH, Chang KH, et al. CT and MR imaging of head and neck tuberculosis. *RadioGraphics* 1997; 17:391–402.
108. Helm CJ, Holland GN. Ocular tuberculosis. *Surv Ophthalmol* 1993; 38:229–256.